

Non-conservation and conservation for different formulations of moist potential vorticity

Parvathi Kooloth¹ | Leslie M. Smith^{2,3} | Samuel N. Stechmann^{2,3}

¹Atmospheric, Climate, & Earth Sciences Division, Pacific Northwest National Laboratory, Richland, Washington, USA

²Department of Mathematics, University of Wisconsin–Madison, Madison, Wisconsin, USA

³Department of Atmospheric and Oceanic Sciences, University of Wisconsin–Madison, Madison, Wisconsin, USA

Correspondence

Parvathi Kooloth, Atmospheric Sciences and Global Change Division, Pacific Northwest National Laboratory, Richland, WA, 99354, USA.
Email: parvathi.kooloth@pnnl.gov

Funding information

Division of Mathematical Sciences, Grant/Award Number: DMS-1907667

Abstract

Potential vorticity (PV) is one of the most important quantities in atmospheric science. In the absence of dissipative processes, the PV of each fluid parcel is known to be conserved, for a dry atmosphere. However, a parcel's PV is not conserved if clouds or phase changes of water occur. Recently, PV conservation laws were derived for a cloudy atmosphere, where each parcel's PV is not conserved but parcel-integrated PV is conserved, for integrals over certain volumes that move with the flow. Hence a variety of different statements are now possible for moist PV conservation and non-conservation, and in comparison to the case of a dry atmosphere, the situation for moist PV is more complex. Here, in light of this complexity, several different definitions of moist PV are compared for a cloudy atmosphere. Numerical simulations are shown for a rising thermal, both before and after the formation of a cloud. These simulations include the first computational illustration of the parcel-integrated, moist PV conservation laws. The comparisons, both theoretical and numerical, serve to clarify and highlight the different statements of conservation and non-conservation that arise for different definitions of moist PV.

KEYWORDS

clouds, conservation law, latent heating, moist potential vorticity, phase changes, water vapor

1 | INTRODUCTION

Potential vorticity (PV) is one of the central conserved quantities in geophysical fluid dynamics (Müller, 1995; Salmon, 1998), with its roots traced back to about a century ago in the works of Rossby (1939) and Ertel (1942). The PV conservation law also has a deep connection to the classic Kelvin and Bjerknes' circulation theorems (Bjerknes, 1898; Thomson, 1867; Thorpe et al., 2003). Material conservation enables the use of PV as a tracer of fluid parcels. PV also possesses an inversion principle

that allows one to recover the slowly varying component of the wind and temperature fields from the PV distribution, with suitable balance relations and boundary conditions (Hoskins et al., 1985; Martin, 2013). Owing to these properties, PV has been used extensively to study the dynamics of synoptic and mesoscale weather systems (Davis & Emanuel, 1991; Hoskins et al., 1985; Lackmann, 2002; Thorpe, 1985) and also ocean circulations (Holland et al., 1984; Marshall & Nurser, 1992; Pollard & Regier, 1990; Rhines, 1986; Ruan et al., 2021; Taylor & Ferrari, 2010).

This is an open access article under the terms of the [Creative Commons Attribution](https://creativecommons.org/licenses/by/4.0/) License, which permits use, distribution and reproduction in any medium, provided the original work is properly cited.

© 2024 The Authors. *Atmospheric Science Letters* published by John Wiley & Sons Ltd on behalf of the Royal Meteorological Society.

Moist versions of PV have also been proposed and investigated extensively (Bennetts & Hoskins, 1979; Emanuel, 1979; Marquet, 2014; Schubert et al., 2001; Wetzel et al., 2019, 2020). Moist PV has been useful for many purposes, including the diagnosis of the effects of latent heating (Abbott & O’Gorman, 2024; Bennetts & Hoskins, 1979; Brennan & Lackmann, 2005; Büeler & Pfahl, 2017; Cao & Cho, 1995; Davis & Emanuel, 1991; Emanuel, 1979; Emanuel, 2008; Gao et al., 2004; Hittmeir et al., 2021; Korty & Schneider, 2007; Lackmann, 2002; Lackmann, 2011; Madonna et al., 2014; Martin, 2013).

Note, though, that moist PV is not conserved for each fluid parcel, and inversion of moist PV is problematic (e.g., see the sequence of three studies of Cao & Cho, 1995; Schubert et al., 2001; Wetzel et al., 2020). The traditional conservation and inversion properties of dry PV are for idealized single-component flows, not for the more realistic cases of binary or multi-component fluids such as a moist atmosphere with clouds and phase changes, and salty oceans.

For inversion, the moist case is different than the dry case in several ways. For instance, the balanced portion is comprised of not one but two components (PV and M, where M represents a slow moist component), and correspondingly it is not PV inversion but PV-and-M inversion that recovers the balanced portion of the system (Remond-Tiedrez et al., 2023; Smith & Stechmann, 2017; Wetzel et al., 2019, 2020). Also, among many different moist PV quantities that have been used, only certain moist PV quantities are slowly evolving in the presence of phase changes of water and cloud latent heating (Wetzel et al., 2020; Zhang et al., 2021a, 2021b, 2022).

For conservation, recently, we generalized the PV conservation laws to cases with phase changes of water, for both a compressible flow (Kooloth et al., 2022) and a Boussinesq flow (Kooloth et al., 2023). We showed that moist PV is not materially conserved as in a dry atmosphere; instead it is conserved over certain ‘material’ volumes that move with flow. Such conservation laws hold for many, but not all, moist PV quantities.

The purpose of this letter is to present a detailed comparison of different statements of PV conservation and non-conservation for various definitions of moist PV. One part of this comparison is the first numerical illustration of the parcel-integrated PV conservation law. From these comparisons, we hope to bring some clarity to the complex landscape of cases including dry versus moist PV, conservation and non-conservation, and parcel-wise versus parcel-integrated conservation.

In what follows, the equations of PV conservation and non-conservation are described for a compressible atmosphere (Section 2) and under the Boussinesq approximation (Section 3). The setup of the numerical simulation

and the simulation results are also presented in Section 3. Finally, Section 4 includes a concluding discussion and summary of the laws of conservation and non-conservation.

2 | COMPARISON OF PV CONSERVATION LAWS

In this section, we compare a variety of statements of conservation and non-conservation of moist potential vorticity, including recently discovered conservation laws that apply for binary or multi-component fluids such as an ocean with salinity or an atmosphere with water vapor, and even in the presence of phase changes and clouds (Kooloth et al., 2022, 2023).

The dry case without water vapor is considered in Section 2.1, where PV is conserved for each fluid parcel. Then the moist case with clouds and phase changes is considered, where each fluid parcel’s PV is not conserved (Section 2.2), but where a local-volume-integrated PV is conserved (Section 2.3).

The setting in this section is a compressible atmosphere. See Section 3 below for an alternative setting under the Boussinesq approximation.

For the evolution equations and assumptions, for velocity $\vec{u} = (u, v, w)$ and density ρ , the form of the equations is the same for both the dry and moist cases:

$$\frac{D\vec{u}}{Dt} = -\frac{1}{\rho}\nabla p + \nabla\phi, \quad \frac{D\rho}{Dt} = -\rho\nabla\cdot\vec{u}, \quad (1)$$

where $\nabla = (\partial_x, \partial_y, \partial_z)$ is the gradient operator, $D/Dt = \partial/\partial t + \vec{u}\cdot\nabla$ is the material derivative, p is the pressure and ϕ is the force potential, which could include, for example, the gravitational potential. In Equation (1) a case without dissipation (friction, viscosity, etc.) is assumed. Rotation could be added with some modifications (Kooloth et al., 2022) but is left out for simplicity here. Also, in Equation (1), the density ρ and pressure p should be interpreted as total density and total pressure, for the dry case and also for the moist case, so that the form of Equation (1) is the same in both cases. To complete the specification of the dynamical evolution, equations are also needed for thermodynamic quantities.

For a dry atmosphere, the thermodynamic evolution equation can be described in terms of potential temperature θ as

$$\frac{D\theta}{Dt} = 0, \quad (2)$$

and an equation of state, $\theta = \theta(p, \rho)$. The evolution is assumed to be (dry) adiabatic.

For a moist (and possibly cloudy) atmosphere, the thermodynamic evolution equations can be described in terms of equivalent potential temperature θ_e and total water specific humidity q_t as

$$\frac{D\theta_e}{Dt} = 0, \quad \frac{Dq_t}{Dt} = 0, \quad (3)$$

along with an equation of state, $\theta_e = \theta_e(p, \rho, q_t)$. The evolution is assumed to be (moist) adiabatic, with reversible phase changes between water vapor and liquid water, as in warm, liquid clouds. No rain, ice, or precipitation is considered. The total water q_t can be decomposed as $q_t = q_v + q_l$, where q_v and q_l are water vapor and liquid water, respectively, and can be recovered from q_t by comparison against the saturation specific humidity, $q_{vs} = q_{vs}(T, p)$, where T is temperature. We refer to states with $q_t < q_{vs}$ and $q_t \geq q_{vs}$ as the unsaturated and saturated phases, respectively.

In what follows, we consider various definitions of moist PV that have been proposed in the past. All definitions involve the vorticity, $\vec{\omega} = \nabla \times \vec{u}$. In analogy with dry PV, $(\vec{\omega} \cdot \nabla \theta) / \rho$, the various moist PV definitions are distinguished by which thermodynamic quantity is used in $\vec{\omega} \cdot \nabla \psi$, where common choices of ψ include potential temperature θ , virtual potential temperature θ_v , equivalent potential temperature θ_e , or liquid water potential temperature θ_l .

2.1 | Dry PV is conserved for each fluid parcel

Dry PV, $(\vec{\omega} \cdot \nabla \theta) / \rho$, is a material invariant—that is, conserved for each fluid parcel. To see this, the starting point is its evolution equation:

$$\begin{aligned} \rho \frac{D}{Dt} \left(\frac{\vec{\omega} \cdot \nabla \theta}{\rho} \right) &= -\nabla \theta \cdot \nabla \times \left(\frac{1}{\rho} \nabla p \right) \\ &= -\nabla \theta \cdot \left(\nabla \frac{1}{\rho} \times \nabla p \right), \end{aligned} \quad (4)$$

which can be derived by using Equations (1) and (2) (see, e.g., Kooloth et al., 2022).

To see that the “solenoidal” term on the right-hand side of Equation (4) is zero for a dry atmosphere, recall a fundamental property of thermodynamics for a dry atmosphere: the potential temperature (or any other thermodynamic property) can be expressed as a function of pressure and density only, so that $\theta = \theta(p, \rho)$. Consequently, we have

$$\nabla \theta = \frac{\partial \theta}{\partial p} \nabla p + \frac{\partial \theta}{\partial \rho} \nabla \rho, \quad (5)$$

and it follows that the right-hand side of Equation (4) is zero, so that

$$\frac{D}{Dt} \left(\frac{\vec{\omega} \cdot \nabla \theta}{\rho} \right) = 0. \quad (6)$$

Hence, dry PV is conserved for each fluid parcel.

2.2 | Moist PV is not conserved for each parcel, due to clouds

We now describe several common choices of moist PV definitions (based on θ , θ_v , θ_e , and θ_l), and show how each one is not a material invariant, in the presence of clouds and phase changes.

As a way to encapsulate any definition of moist PV, consider a moist PV defined as $(\vec{\omega} \cdot \nabla \psi) / \rho$, for a generic thermodynamic quantity ψ . Assume that the evolution of ψ is given by $D\psi/Dt = \dot{\psi}$, where $\dot{\psi}$ represents all sources/sinks of ψ . Then the evolution of the generic moist PV is given by

$$\frac{D}{Dt} \left(\frac{\vec{\omega} \cdot \nabla \psi}{\rho} \right) = \frac{1}{\rho^3} \nabla \psi \cdot (\nabla \rho \times \nabla p) + \frac{1}{\rho} \vec{\omega} \cdot \nabla \dot{\psi} \quad (7)$$

which follows from Equation (1) (see, e.g., Kooloth et al., 2022; Schubert et al., 2001). Two potential sources of non-conservation appear on the right-hand side in Equation (7): the “solenoidal” term involving a cross product and the source term involving $\dot{\psi}$.

First choose $\psi = \theta$ and consider PV_θ based on potential temperature. From Equation (7) its evolution equation is

$$\frac{D}{Dt} \left(\frac{\vec{\omega} \cdot \nabla \theta}{\rho} \right) = \frac{1}{\rho^3} \nabla \theta \cdot (\nabla \rho \times \nabla p) + \frac{1}{\rho} \vec{\omega} \cdot \nabla \dot{\theta}. \quad (8)$$

In an atmosphere with clouds and phase changes, Equation (8) cannot be further simplified. The $\dot{\theta}$ term arises from cloud latent heating and does not vanish, and the solenoidal term on the right hand side of Equation (8) remains nonzero in Equation (8), since, for a moist atmosphere with phase changes, the potential temperature is no longer completely determined by only the two variables of pressure and density, since three variables are typically needed to specify a thermodynamic relationship

in a moist setting (see, e.g., chapter 4 of Iribarne & Godson, 1973; Ooyama, 2001; Pauluis, 2008). Consequently, PV_θ is not a material invariant if clouds and phase changes are present.

Next consider PV_{θ_v} based on the virtual potential temperature θ_v . Its evolution equation is

$$\frac{D}{Dt} \left(\frac{\vec{\omega} \cdot \nabla \theta_v}{\rho} \right) = \frac{1}{\rho} \vec{\omega} \cdot \nabla \dot{\theta}_v, \quad (9)$$

which follows from choosing $\psi = \theta_v$ in Equation (7). The solenoidal term from Equation (7) has vanished and does not appear in Equation (9), which is one of the desirable properties of PV_{θ_v} (Schubert et al., 2001). It vanishes because θ_v is a special quantity that is a function of the two variables p and ρ alone: $\theta_v = T_v(p_0/p)^{R_d/c_{pd}}$, where virtual temperature is $T_v = p/(\rho R_d)$, and the constants are the reference pressure p_0 , gas constant R_d for dry air and specific heat c_{pd} at constant pressure for dry air. The right hand side of Equation (9) still has a source term resulting from non-conservation of θ_v , such as cloud latent heating, so that PV_{θ_v} is not a material invariant in general. As a special case, though, while a parcel remains in the unsaturated phase, we have $\dot{\theta}_v = 0$ due to the absence of latent heating, and consequently PV_{θ_v} remains materially conserved in the unsaturated phase.

Another commonly used definition of moist potential vorticity is PV_{θ_e} defined in terms of the equivalent potential temperature θ_e . Note that θ_e is often assumed to be a materially conserved quantity, that is, $D\theta_e/Dt = 0$. Hence, from Equation (7), the evolution of PV_{θ_e} is given by

$$\frac{D}{Dt} \left(\frac{\vec{\omega} \cdot \nabla \theta_e}{\rho} \right) = \frac{1}{\rho^3} \nabla \theta_e \cdot (\nabla \rho \times \nabla p). \quad (10)$$

Here, in the case of PV_{θ_e} , the non-conservation is due to the solenoidal term.

As a final common choice, one may also consider potential vorticity PV_{θ_l} defined in terms of liquid water potential temperature θ_l . Note that θ_l is often assumed to be a materially conserved quantity, that is, $D\theta_l/Dt = 0$ (e.g., Betts, 1973; Stevens, 2005). Hence, from Equation (7), the evolution of PV_{θ_l} is given by

$$\frac{D}{Dt} \left(\frac{\vec{\omega} \cdot \nabla \theta_l}{\rho} \right) = \frac{1}{\rho^3} \nabla \theta_l \cdot (\nabla \rho \times \nabla p), \quad (11)$$

and non-conservation of PV_{θ_l} is seen to be due to the solenoidal term.

Note that the PV evolution would be in the form of Equations (10) and (11) for any PV_ψ based on a thermodynamic quantity ψ that is assumed to be conserved ($D\psi/Dt = 0$), including, for example, entropy s or the moist potential temperature θ_s proposed by Marquet (2011, 2014). For further discussion, see Supporting Information (SI) Section 1.

In summary, the four moist PVs here involve four common potential temperature variables: θ , θ_v , θ_e , and θ_l . The discussion above serves to illustrate the different properties of the four cases. They are all non-conservative in different ways, due to either sources/sinks or the solenoidal term. For instance, θ_v has a source term due to cloud latent heating, so PV_{θ_v} is conserved (a material invariant) in the unsaturated phase but is not conserved in the saturated phase. On the other hand, the variables θ_e and θ_l are conserved, so non-conservation of PV_{θ_e} and PV_{θ_l} is due to the solenoidal term only. Hence, it appears that there may not be a moist PV quantity that is a material invariant, due to clouds and phase changes.

2.3 | Moist PV is conserved over certain local volumes, even with clouds

While moist PV may be non-conservative for each fluid parcel, it has been recently shown by Kooloth et al. (2022, 2023) that moist PV can be conserved when integrated over certain local volumes (for PV_{θ_e} or PV_{θ_l} , but not PV_θ or PV_{θ_v}). Here we sketch the key ideas of these conservation principles.

As motivation for integrating over local volumes, start with the PV_{θ_e} evolution equation in Equation (10), rewritten as¹

$$\rho \frac{D}{Dt} \left(\frac{\vec{\omega} \cdot \nabla \theta_e}{\rho} \right) = \nabla \cdot \left[\frac{1}{\rho} \nabla \times (\theta_e \nabla p) \right]. \quad (12)$$

Given that a divergence appears on the right-hand side, one might try to integrate in order to remove this divergence term.

Pursuing this direction, we integrate Equation (12) over a material volume² V_m (i.e., a volume that moves with the fluid flow) and use the divergence theorem to arrive at

$$\frac{d}{dt} \iiint_{V_m} dV (\vec{\omega} \cdot \nabla \theta_e) = \oint_{S_m} d\vec{S} \cdot \left(\frac{1}{\rho} \nabla \theta_e \times \nabla p \right) \quad (13)$$

where S_m is the material surface that bounds the material volume. The right-hand side is still non-zero, so conservation has not yet been demonstrated.

To simplify the right-hand side of Equation (13), first choose the material volume V_m to be a distorted cylinder with base and lid given by surfaces of constant θ_e (say $\theta_e = \theta_{e1}$ and $\theta_e = \theta_{e2}$, respectively) and sides given by $q_t = q_t(\theta_e)$. (An illustration of such a cylinder is shown below in Section 3.) On the base and lid, $d\vec{S} \parallel \nabla\theta_e$ that is, the normal to the surface is parallel to $\nabla\theta_e$, so the base and lid provide zero contribution to the integral. Therefore the surface integral over S_m is the same as a surface integral over only the sides of the cylinder:

$$\oint_{S_m} d\vec{S} \cdot \left(\frac{1}{\rho} \nabla\theta_e \times \nabla p \right) = \iint_{S_{\text{sides}}} d\vec{S} \cdot \left(\frac{1}{\rho} \nabla\theta_e \times \nabla p \right) \quad (14)$$

$$= - \iint_{S_{\text{sides}}} d\vec{S} \cdot \nabla \times (g(p, \theta_e) \nabla p). \quad (15)$$

Also, to obtain the last line above, a second key observation, from fundamentals of moist thermodynamics, is needed: ρ can be written as $\rho = \rho(p, \theta_e, q_t)$ as a function of the three moist thermodynamic quantities (p, θ_e, q_t) (e.g., chapter 4 of Iribarne & Godson, 1973; Ooyama, 2001; Pauluis, 2008). Furthermore, since $q_t = q_t(\theta_e)$ on the sides of the cylinder, we have $\rho = \rho(p, \theta_e, q_t(\theta_e))$ and ρ is a function of p and θ_e alone. It follows that the integrands of Equations (14) and (15) are equal for a function $g(p, \theta_e)$ that satisfies $\partial g / \partial \theta_e = 1 / \rho(p, \theta_e, q_t(\theta_e))$.

To complete the derivation, by using Stokes theorem, the surface integral in Equation (15) can be converted to two closed line integrals along the edges of the cylinder, C_1 and C_2 , and we have

$$\frac{d}{dt} \iiint_{V_m} dV (\vec{\omega} \cdot \nabla \theta_e) = - \oint_{C_1} d\vec{x} \cdot (g(p, \theta_e) \nabla p) + \oint_{C_2} d\vec{x} \cdot (g(p, \theta_e) \nabla p). \quad (16)$$

By noting that θ_e is a constant on both C_1 and C_2 , the integrands above reduce to exact differentials which integrate to zero on the closed curves. This gives us our final result,

$$\frac{d}{dt} \iiint_{V_m} \frac{\vec{\omega} \cdot \nabla \theta_e}{\rho} \rho dV = 0, \quad (17)$$

of conservation of PV_{θ_e} when integrated over certain local material volumes.³

A similar conservation law can be derived for PV_{θ_i} or PV based on entropy or even PV_{q_t} (Kooloth et al., 2022). The key property shared by θ_e , θ_i , s (entropy), and q_t is that they are all material invariants. On the other hand, θ

and θ_v are not material invariants in the presence of phase changes and clouds, and hence the derivation above does not hold for PV_{θ} or PV_{θ_v} .

3 | NUMERICAL SIMULATIONS OF PV CONSERVATION AND NONCONSERVATION

For numerical demonstration of the conservation laws from Section 2, we will set aside the compressible setting that includes acoustic/sound waves and use the simpler setting of the Boussinesq approximation. The governing equations under the Boussinesq approximation are described in the SI, and they are similar to equations of moist Boussinesq dynamics that have been used in other studies (e.g., Bretherton, 1987; Grabowski & Clark, 1993; Hernandez-Duenas et al., 2013; Kuo, 1961; Marsico et al., 2019; Pauluis & Schumacher, 2010; Stechmann, 2014; Stechmann & Stevens, 2010). The Boussinesq case admits statements of PV conservation and non-conservation (Kooloth et al., 2023) that are analogous to the compressible case from Section 2. Details are described in SI Section 2. A summary is as follows.

As a particular moist PV quantity for illustration, we use PV_u which is based on the total buoyancy b_u in the unsaturated phase:

$$PV_u = \vec{\omega} \cdot \nabla b_u. \quad (18)$$

The evolution of PV_u is then given by

$$\frac{D}{Dt} PV_u = \frac{D}{Dt} (\vec{\omega} \cdot \nabla b_u) = \nabla b_u \cdot (\nabla \times b' \hat{z}). \quad (19)$$

The buoyancy b' depends on the phase and is nonconservative; see the SI for its detailed definition. Consequently, it appears as a source term in the evolution of PV_u , which is then also nonconservative.

As a special case, though, note that the right-hand-side goes to zero in the unsaturated phase since $\nabla b_u \cdot (\nabla \times b_u H_u \hat{z}) = 0$, and therefore

$$\frac{D}{Dt} PV_u = \frac{D}{Dt} (\vec{\omega} \cdot \nabla b_u) = 0 \quad \text{if unsaturated}, \quad (20)$$

so that PV_u is materially conserved for any parcels that are not inside a cloud.

For a general scenario involving phase changes, following similar steps as presented for the compressible case in Section 2.3, a parcel-integrated PV_u conservation principle can be obtained:

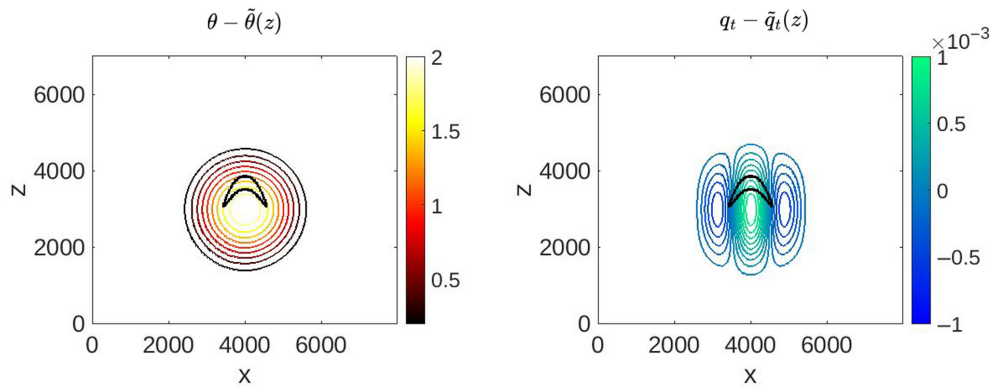


FIGURE 1 Initial conditions for the 3D rising thermal. Plots are shown in the (x, z) plane with fixed $y = 0.5L_y = 3500$ m. Anomalies of potential temperature θ (left) and total water specific humidity q_t (right), defined as anomalies from a horizontally uniform background state, $\tilde{\theta}(z)$ and $\tilde{q}_t(z)$. The units for x and z are meters, and the units for θ and q_t are K and kg/kg respectively. The black closed curve represents the vertical cross-section of the material volume V_m considered in Section 3.1.

$$\frac{d}{dt} \iiint_{V_m} \vec{\omega} \cdot \nabla b_u dV = 0, \quad (21)$$

which follows from integrating Equation (19) over a material volume V_m that is a distorted cylinder whose base and lid are given by $b_u = \text{const.}$ and the sides are given by $b_s = \text{const.}$, where b_s is the total buoyancy in the saturated phase. This PV_u conservation statement can also be shown to be valid for a material volume enclosed by isosurfaces of the more physically relevant quantities, θ_e and q_t . The main ideas of the derivation are the same as in the compressible case; the interested reader can refer to the SI for the detailed derivation.

Parcel-integrated conservation principles can also be derived for many other potential vorticity quantities for the Boussinesq system. One such quantity is potential vorticity $PV_s = \vec{\omega} \cdot \nabla b_s$ based on the total saturated buoyancy; two others are $PV_e = \vec{\omega} \cdot \nabla \theta_e$ based on equivalent potential temperature θ_e , and $PV_l = \vec{\omega} \cdot \nabla \theta_l$ based on liquid water potential temperature θ_l . Additionally, it can be shown that PV_s is materially conserved in the saturated phase using a similar reasoning as for PV_u in the unsaturated phase (Kooloth et al., 2023).

The three-dimensional (3D) numerical simulations in this study are performed using the code of Hernandez-Duenas et al. (2013). The channel domain is periodic in the x and y directions, and assumes a rigid top and bottom. The domain size $L_x \times L_y \times H$ is $8000 \times 8000 \times 7000$ m³ and the number of grid points is $256 \times 256 \times 400$, corresponding to horizontal and vertical grid spacings of 31.5 m and 17.5 m, respectively. Additional details are described in SI Sections 3 and 4 and Figures S1.

The case study for illustration is the well-known case of a rising moist thermal (e.g., Ahmad & Lindeman, 2007;

Carpenter Jr et al., 1990; Grabowski & Clark, 1991, 1993; Lilly, 1962; Morrison et al., 2021). Details of the setup are described in SI section 3. The basic aspects of the simulation are as follows. A vertical slice through the initial, unsaturated perturbation is shown in Figure 1 (at $y = 3500$ m). At $t = 0$, the velocity is zero, and the perturbation potential temperature is spherically symmetric, while the perturbation in q_t is non-spherical in order to allow PV_u to be generated according to the PV_u source term in Equation (19). Evolution of the perturbation in a (x, z) plane is shown in Figure 2. For $t > 0$, the warm bubble rises due to its buoyancy and a non-zero velocity field develops. In the plane at $y = 3500$ m, the vapor starts to condense near the center of the plane at $t \approx 1.8$ min, contributing to the formation of a 3D cloud (Figures 2 and 3). The size of the cloud grows as more fluid parcels change phase (see Figure 2 at $t = 3$ min and Figure 3 at $t = 1.2$ min).

3.1 | Local-volume integrated PV_u conservation

In order to verify volume-integrated PV_u conservation, a material volume is identified and tracked over time in the rising bubble simulation described above. The material volume consists of roughly 29,500 grid cells and is specified by certain level surfaces for θ_e and q_t , such that their intersection encloses a moving material volume. As shown in Figure 3, at an early time of $t = 0.3$ min, the fluid parcels in the material volume are unsaturated. By the later time of $t = 1.2$ min, however, a cloud has developed in upper levels of the volume, and 31% of the fluid parcels within the material volume have undergone a change of phase in their water content, from water vapor

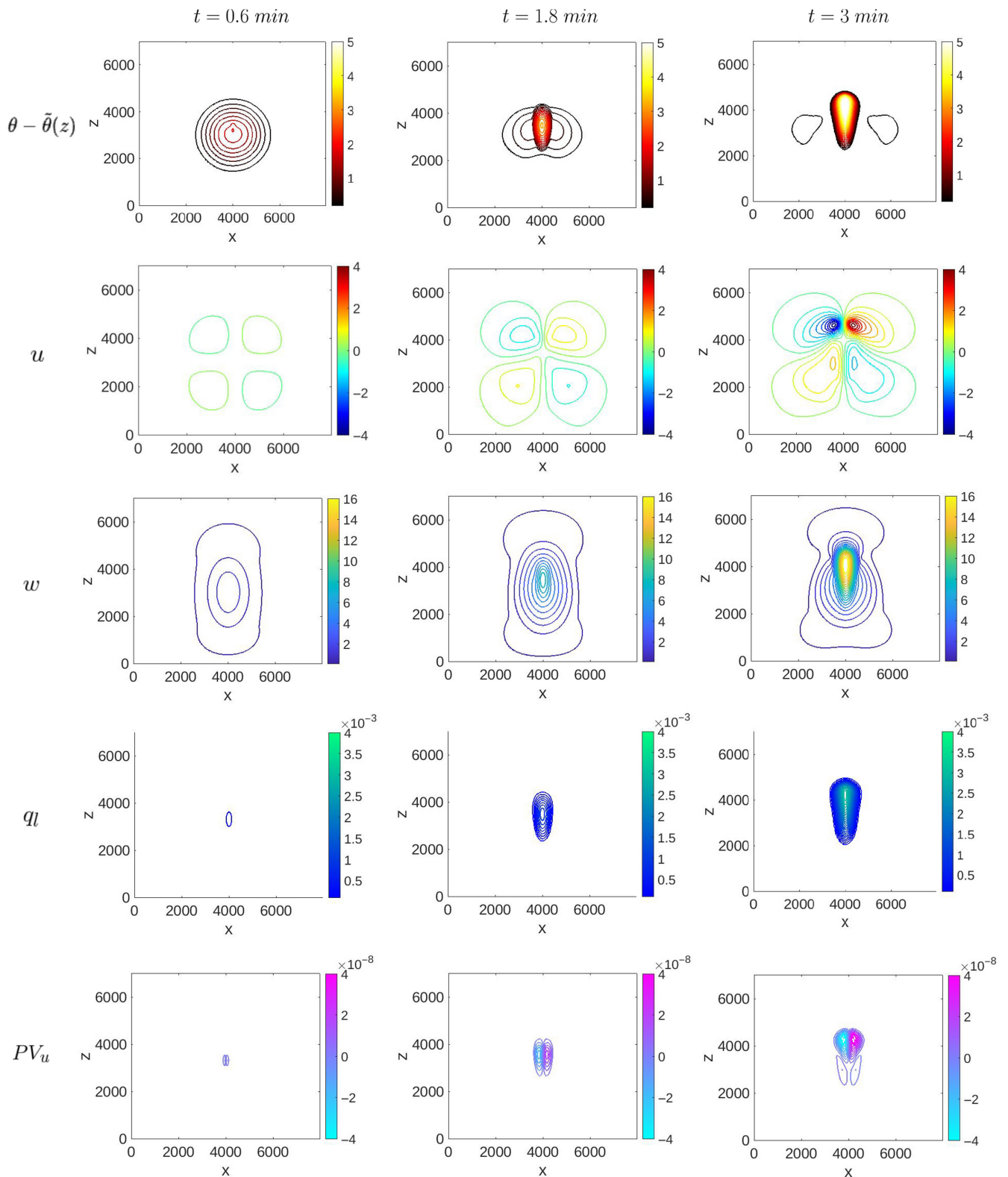


FIGURE 2 Snapshots of the warm bubble in the plane with fixed $y = 0.5L_y$ m. Rows show $\theta - \tilde{\theta}$, u , w , q_l and PV_u and columns show times $t = 0.6, 1.8$ and 3 minutes. The units for x and z are meters, and the units for θ , velocities (u, v, w), q_l and PV_u are K, m/s, kg/kg and s^{-3} respectively.

to liquid water. Two more times, $t = 3$ min and $t = 4.5$ min, are considered in Figure 3, by which time 99% and 100% of the parcels have become saturated, respectively.

Concurrently, within the cloud, the local values of PV_u are evolving (see Figure 2 and further details in SI Section 4).

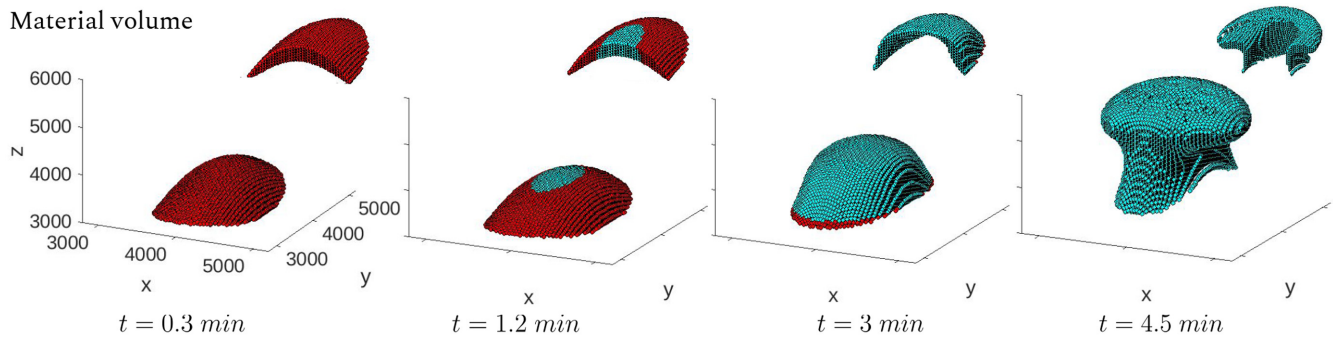


FIGURE 3 Illustration of a material volume, at times $t = 0.3, 1.2, 3$ and 4.5 min. Evolution of a material volume enclosed between $\theta_e > 325.5$ K and $q_t < 6.0 \times 10^{-3}$ (in kg/kg). The inset figures are the vertical cross-sections through the material volumes. The red and the cyan dots represent the unsaturated and saturated parcels respectively.

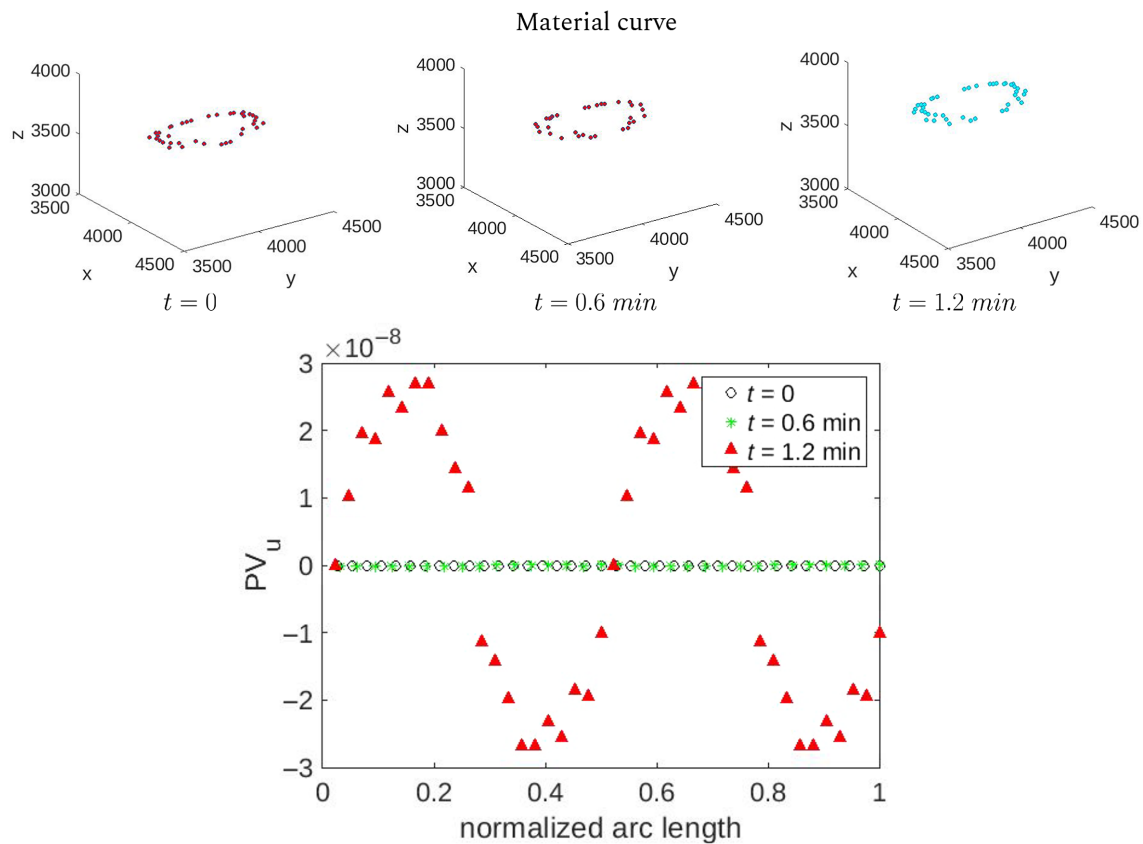


FIGURE 4 Demonstration of parcel-wise non-conservation of PV_u (s^{-1}), due to phase change between $t = 0.6$ and 1.2 min. (Top row) Evolution of a closed material curve of $\theta_e^{tot} \approx 326.48$ K and $q_t^{tot} \approx 0.00566$ kg/kg. (Bottom row) Evolution of PV_u on the closed material curve. The points on the material curve are ordered using the arc length coordinate.

On the other hand, we can numerically check for local volume-integrated PV_u by computing

$$IPV = \iiint_{V_m} dV PV_u, \quad (22)$$

where V_m is the specified material volume. Noting that the initial velocity field is zero everywhere in the domain,

then the IPV starts at the value zero, to machine precision. By monitoring Equation (22), we find that the IPV within the material volume remains small. For instance, at time $t = 1.2$ min, the IPV is $O(10^{-14})$, which is small or negligible in comparison to the maximum PV_u value of $O(10^{-8})$ within the volume. Similarly, at the later time $t = 4.5$ min, the IPV is $O(10^{-12})$, which is small in comparison to the maximum PV_u value of $O(10^{-5})$ within

TABLE 1 Summary of various PV formulations and their conservation, inversion, and balance/slow variation properties.

PV definition	Material invariant	Material-volume-integrated invariant	Inversion ^a	Slowly varying ^b
<i>Dry</i>				
$PV_\theta = \frac{\vec{\omega} \cdot \nabla \theta}{\rho}$	Everywhere	All V_m	PV	Yes
<i>Moist</i>				
$PV_{\theta_v} = \frac{\vec{\omega} \cdot \nabla \theta_v}{\rho}$	Unsaturated phase	All unsaturated V_m	None	No
$PV_{\theta_e} = \frac{\vec{\omega} \cdot \nabla \theta_e}{\rho}$	Nowhere	Certain V_m , even with phase changes	PV-and-M	Yes
$PV_{\theta_l} = \frac{\vec{\omega} \cdot \nabla \theta_l}{\rho}$	Nowhere	Certain V_m , even with phase changes	PV-and-M	Yes
<i>Moist Boussinesq</i>				
$PV_u = \vec{\omega} \cdot \nabla b_u$	Unsaturated phase	Certain V_m , even with phase changes, and also all unsaturated V_m	PV-and-M	Yes
$PV_s = \vec{\omega} \cdot \nabla b_s$	Saturated phase	Certain V_m , even with phase changes, and also all saturated V_m	PV-and-M	Yes
$PV_e = \vec{\omega} \cdot \nabla \theta_e$	nowhere	certain V_m , even with phase changes	PV-and-M	Yes
$PV_l = \vec{\omega} \cdot \nabla \theta_l$	Nowhere	Certain V_m , even with phase changes	PV-and-M	Yes

Note: V_m refers to a material volume.

^aTo recover the balanced or slowly evolving component(s) of the system.

^bWith phase changes in the moist cases.

the volume. Hence, for the duration of the simulation, and given the inherent numerical errors in the simulation, the conservation statement for parcel-integrated PV is verified.

3.2 | Material PV_u conservation and non-conservation

In this section, we investigate the material conservation of PV_u . It is shown that PV_u is materially conserved prior to the time when fluid parcels undergo phase change from vapor to liquid, but not for later times after the cloud has formed. We identify and track a closed material curve within the material volume, which are both rising along with the bubble, as shown on the first row of Figure 4. The material curve is initially unsaturated, but by $t = 1.2$ min, all the parcels composing the material curve have undergone a change of phase.

To quantify material conservation and non-conservation, we measured the maximum of the absolute value of PV_u within the material volume (Figure 3). At representative early time $t = 0.3$, before a significant number of parcels have experienced a change of water phase, the max absolute value of PV_u within the entire material volume is $5.7 \times 10^{-11} \text{ s}^{-3}$. In comparison, at later time $t = 1.2$ min, by which time a robust cloud has formed, the max absolute value of PV_u within the volume has increased by roughly 3 orders of magnitude, to $6.8 \times 10^{-8} \text{ s}^{-3}$.

As a graphical illustration, the bottom row of Figure 4 shows the PV_u values along the selected material curve. The figure shows PV_u associated with each grid point along the curve, at three different times $t = 0, 0.6, 1.2$ minutes. At $t = 0$ and $t = 0.6$ min, when the material curve is unsaturated, the PV_u values are close to zero. At $t = 1.2$ min, some PV_u values associated with the material curve are of the order of 10^{-8} s^{-1} , demonstrating that PV_u does not remain conserved along the material curve once the parcels undergo change of water phase.

4 | CONCLUSIONS

In this work, a main goal was to compare and contrast the different moist PV conservation statements and non-conservation statements, in light of the rich variety of possibilities in the literature, including recent developments (e.g. Bennetts & Hoskins, 1979; Emanuel, 1979; Kooloth et al., 2022, 2023; Marquet, 2014; Schubert et al., 2001).

As a summary, Table 1 lists the different formulations of PV considered here and their conservation laws. We note that in a moist flow with phase changes, there are no material invariant PVs; the strongest conservation principle realizable in this setting is an integrated PV invariance for certain material volumes. In both the fully compressible and Boussinesq cases, PVs based on θ_e and θ_l possess a material-volume-integrated conservation principle, even with phase transitions. In the moist

Boussinesq setting, PV_u and PV_s , based on the unsaturated and saturated buoyancy, respectively, also have an integrated PV invariance principle within certain material volumes even with phase changes. Additionally, as special cases, PV_u and PV_s remain materially invariant in the unsaturated and saturated phases respectively.

A more complete set of desirable properties is often associated with PV, including conservation, inversion, and balance/slow variation. Table 1 also summarizes these other properties. As one note about inversion and balance/slow variation, since PV_{θ_v} is not slowly varying, any inversion with PV_{θ_v} will not completely remove the fast wave contributions in the presence of phase changes (Wetzel et al., 2020). The moist PV quantities that are defined in terms of conserved thermodynamic variables (e.g., θ_e or θ_l or entropy s) are slowly evolving, and they are associated with a PV-and-M inversion principle (see the discussion of inversion in Section 1, and associated references such as Wetzel et al. (2020)).

One application of parcel-integrated PV conservation laws is for diagnosing diabatic processes in the atmosphere or ocean (see discussion in Section 1). In the past, (parcel-wise) PV non-conservation was often used to indicate cloud latent heating, as a leading diabatic process. In contrast, for the new conservation laws of PV as a parcel-integrated invariant, the conservation law holds even in the presence of phase changes and cloud latent heating; consequently, any non-conservation must be due to other diabatic processes, such as friction/viscosity, radiative cooling/heating, or precipitation. Therefore, the parcel-integrated conservation laws can potentially provide new information about other diabatic processes in diagnostic studies.

AUTHOR CONTRIBUTIONS

Parvathi Kooloth: Conceptualization; data curation; formal analysis; investigation; methodology; visualization; writing – original draft; writing – review and editing. **Leslie M. Smith:** Conceptualization; data curation; formal analysis; investigation; methodology; supervision; visualization; writing – original draft; writing – review and editing. **Samuel N. Stechmann:** Conceptualization; data curation; formal analysis; investigation; methodology; supervision; visualization; writing – original draft; writing – review and editing.

ACKNOWLEDGEMENTS

The authors thank three anonymous reviewers for helpful comments, and Gerardo Hernandez-Duenas for providing the computer code used for the simulations. L.M. Smith and S.N. Stechmann gratefully acknowledge support from US NSF grant DMS-1907667.

CONFLICT OF INTEREST STATEMENT

The authors declare no conflicts of interest.

DATA AVAILABILITY STATEMENT

Data available on request from the authors.

ENDNOTES

¹ Using vector calculus identities, note that $-\nabla\theta_e \cdot \nabla \times \left(\frac{1}{\rho} \nabla p \right) = -\nabla\theta_e \cdot \nabla_{\rho}^{\perp} \times \nabla p = \nabla_{\rho}^{\perp} \cdot \nabla\theta_e \times \nabla p = \nabla_{\rho}^{\perp} \cdot \nabla \times (\theta_e \nabla p) = \nabla \cdot \left[\frac{1}{\rho} \nabla \times (\theta_e \nabla p) \right]$.

² Recall that, for a material volume, we have $\frac{d}{dt} \int_{V_m} dV \left(\vec{\omega} \cdot \nabla\theta_e \right) = \int_{V_m} dV \rho \frac{D}{Dt} \left(\frac{\vec{\omega} \cdot \nabla\theta_e}{\rho} \right)$.

³ It is an open question to understand how general the material volumes could be. See Kooloth et al. (2022, 2023) for some other known examples.

REFERENCES

- Abbott, T.H. & O’Gorman, P.A. (2024) Impact of precipitation mass sinks on midlatitude storms over a wide range of climates. submitted.
- Ahmad, N. & Lindeman, J. (2007) Euler solutions using flux-based wave decomposition. *International Journal for Numerical Methods in Fluids*, 54, 47–72.
- Bennetts, D.A. & Hoskins, B. (1979) Conditional symmetric instability—a possible explanation for frontal rainbands. *Quarterly Journal of the Royal Meteorological Society*, 105, 945–962.
- Betts, A. (1973) Non-precipitating cumulus convection and its parameterization. *Quarterly Journal of the Royal Meteorological Society*, 99, 178–196.
- Bjerknes, V. (1898) Über einen hydrodynamischen zirkulationssatz und seine anwendung auf die mechanik der atmosphäre und des weltmeeres. *Kungliga Svenska Vetenskapsakademiens Handlingar*, 31, 97–106.
- Brennan, M.J. & Lackmann, G.M. (2005) The influence of incipient latent heat release on the precipitation distribution of the 24–25 January 2000 us east coast cyclone. *Monthly Weather Review*, 133, 1913–1937.
- Bretherton, C.S. (1987) A theory for nonprecipitating moist convection between two parallel plates. Part I: thermodynamics and “linear” solutions. *Journal of Atmospheric Sciences*, 44, 1809–1827.
- Büeler, D. & Pfahl, S. (2017) Potential vorticity diagnostics to quantify effects of latent heating in extratropical cyclones. Part I: methodology. *Journal of the Atmospheric Sciences*, 74, 3567–3590.
- Cao, Z. & Cho, H.-R. (1995) Generation of moist potential vorticity in extratropical cyclones. *Journal of the Atmospheric Sciences*, 52, 3263–3282.
- Carpenter, R.L., Jr., Droegemeier, K.K., Woodward, P.R. & Hane, C.E. (1990) Application of the piecewise parabolic method (PPM) to meteorological modeling. *Monthly Weather Review*, 118, 586–612.
- Davis, C.A. & Emanuel, K.A. (1991) Potential vorticity diagnostics of cyclogenesis. *Monthly Weather Review*, 119, 1929–1953.
- Emanuel, K. (2008) Back to Norway: an essay. In: *Synoptic-dynamic meteorology and weather analysis and forecasting: a tribute to fred sanders*. Boston, MA: Springer, pp. 87–96.

- Emanuel, K.A. (1979) Inertial instability and mesoscale convective systems. Part I: linear theory of inertial instability in rotating viscous fluids. *Journal of the Atmospheric Sciences*, 36, 2425–2449.
- Ertel, H. (1942) Ein neuer hydrodynamischer wirbelsatz. *Meteorologische Zeitschrift*, 59, 277–281.
- Gao, S., Wang, X. & Zhou, Y. (2004) Generation of generalized moist potential vorticity in a frictionless and moist adiabatic flow. *Geophysical Research Letters*, 31.
- Grabowski, W.W. & Clark, T.L. (1991) Cloud–environment interface instability: rising thermal calculations in two spatial dimensions. *Journal of the Atmospheric Sciences*, 48, 527–546.
- Grabowski, W.W. & Clark, T.L. (1993) Cloud–environment interface instability: part II: extension to three spatial dimensions. *Journal of the Atmospheric Sciences*, 50, 555–573.
- Hernandez-Duenas, G., Majda, A.J., Smith, L.M. & Stechmann, S.N. (2013) Minimal models for precipitating turbulent convection. *Journal of Fluid Mechanics*, 717, 576–611.
- Hittmeir, S., Klein, R., Müller, A. & Névir, P. (2021) The dynamic state index with moisture and phase changes. *Journal of Mathematical Physics*, 62, 123101.
- Holland, W., Keffer, T. & Rhines, P. (1984) Dynamics of the oceanic general circulation: the potential vorticity field. *Nature*, 308, 698–705.
- Hoskins, B.J., McIntyre, M.E. & Robertson, A.W. (1985) On the use and significance of isentropic potential vorticity maps. *Quarterly Journal of the Royal Meteorological Society*, 111, 877–946.
- Iribarne, J. & Godson, W. (1973) *Atmospheric thermodynamics*. Boston: D. Reidel Publishing Company.
- Kooloth, P., Smith, L.M. & Stechmann, S.N. (2022) Conservation laws for potential vorticity in a salty ocean or cloudy atmosphere. *Geophysical Research Letters*, 49, e2022GL100009.
- Kooloth, P., Smith, L.M. & Stechmann, S.N. (2023) Hamilton's principle with phase changes and conservation principles for moist potential vorticity. *Quarterly Journal of the Royal Meteorological Society*, 149, 1056–1072.
- Korty, R.L. & Schneider, T. (2007) A climatology of the tropospheric thermal stratification using saturation potential vorticity. *Journal of Climate*, 20, 5977–5991.
- Kuo, H. (1961) Convection in conditionally unstable atmosphere. *Tellus*, 13, 441–459.
- Lackmann, G. (2011) *Midlatitude synoptic meteorology: dynamics*. Boston, USA: Analysis, and Forecasting.
- Lackmann, G.M. (2002) Cold-frontal potential vorticity maxima, the low-level jet, and moisture transport in extratropical cyclones. *Monthly Weather Review*, 130, 59–74.
- Lilly, D.K. (1962) On the numerical simulation of buoyant convection. *Tellus*, 14, 148–172.
- Madonna, E., Wernli, H., Joos, H. & Martius, O. (2014) Warm conveyor belts in the era-interim dataset (1979–2010). Part I: climatology and potential vorticity evolution. *Journal of Climate*, 27, 3–26.
- Marquet, P. (2011) Definition of a moist entropy potential temperature: application to FIRE-I data flights. *Quarterly Journal of the Royal Meteorological Society*, 137, 768–791.
- Marquet, P. (2014) On the definition of a moist-air potential vorticity. *Quarterly Journal of the Royal Meteorological Society*, 140, 917–929.
- Marshall, J.C. & Nurser, A.G. (1992) Fluid dynamics of oceanic thermocline ventilation. *Journal of Physical Oceanography*, 22, 583–595.
- Marsico, D.H., Smith, L.M. & Stechmann, S.N. (2019) Energy decompositions for moist Boussinesq and anelastic equations with phase changes. *Journal of the Atmospheric Sciences*, 76, 3569–3587.
- Martin, J.E. (2013) *Mid-latitude atmospheric dynamics: a first course*. West Sussex, England: John Wiley & Sons.
- Morrison, H., Peters, J.M. & Sherwood, S.C. (2021) Comparing growth rates of simulated moist and dry convective thermals. *Journal of the Atmospheric Sciences*, 78, 797–816.
- Müller, P. (1995) Ertel's potential vorticity theorem in physical oceanography. *Reviews of Geophysics*, 33, 67–97.
- Ooyama, K.V. (2001) A dynamic and thermodynamic foundation for modeling the moist atmosphere with parameterized microphysics. *Journal of the Atmospheric Sciences*, 58, 2073–2102.
- Pauluis, O. (2008) Thermodynamic consistency of the anelastic approximation for a moist atmosphere. *Journal of the Atmospheric Sciences*, 65, 2719–2729.
- Pauluis, O. & Schumacher, J. (2010) Idealized moist Rayleigh–Bénard convection with piecewise linear equation of state. *Communications in Mathematical Sciences*, 8, 295–319.
- Pollard, R. & Regier, L. (1990) Large variations in potential vorticity at small spatial scales in the upper ocean. *Nature*, 348, 227–229.
- Remond-Tiedrez, A., Smith, L.M. & Stechmann, S.N. (2023) A non-linear elliptic PDE from atmospheric science: well-posedness and regularity at cloud edge. *arXiv preprint arXiv:2301.07611*.
- Rhines, P.B. (1986) Vorticity dynamics of the oceanic general circulation. *Annual Review of Fluid Mechanics*, 18, 433–497.
- Rossby, C.-G. (1939) Relation between variations in the intensity of the zonal circulation of the atmosphere and the displacements of the semi-permanent centers of action. *Journal of Marine Research*, 2, 38–55.
- Ruan, X., Thompson, A.F. & Taylor, J.R. (2021) The evolution and arrest of a turbulent stratified oceanic bottom boundary layer over a slope: upslope regime and PV dynamics. *Journal of Physical Oceanography*, 51, 1077–1089.
- Salmon, R. (1998) *Lectures on geophysical fluid dynamics*. New York, USA: Oxford University Press.
- Schubert, W.H., Hausman, S.A., Garcia, M., Ooyama, K.V. & Kuo, H.-C. (2001) Potential vorticity in a moist atmosphere. *Journal of the Atmospheric Sciences*, 58, 3148–3157.
- Smith, L.M. & Stechmann, S.N. (2017) Precipitating quasigeostrophic equations and potential vorticity inversion with phase changes. *Journal of the Atmospheric Sciences*, 74, 3285–3303.
- Stechmann, S.N. (2014) Multiscale eddy simulation for moist atmospheric convection: preliminary investigation. *Journal of Computational Physics*, 271, 99–117.
- Stechmann, S.N. & Stevens, B. (2010) Multiscale models for cumulus cloud dynamics. *Journal of the Atmospheric Sciences*, 67, 3269–3285.
- Stevens, B. (2005) Atmospheric moist convection. *Annual Review of Earth and Planetary Sciences*, 33, 605–643.
- Taylor, J.R. & Ferrari, R. (2010) Buoyancy and wind-driven convection at mixed layer density fronts. *Journal of Physical Oceanography*, 40, 1222–1242.
- Thomson, W. (1867) 4. On vortex atoms. *Proceedings of the Royal Society of Edinburgh*, 6, 94–105.
- Thorpe, A. (1985) Diagnosis of balanced vortex structure using potential vorticity. *Journal of the Atmospheric Sciences*, 42, 397–406.

- Thorpe, A.J., Volkert, H. & Ziemiański, M.J. (2003) The Bjerknes' circulation theorem: a historical perspective: a historical perspective. *Bulletin of the American Meteorological Society*, 84, 471–480.
- Wetzel, A.N., Smith, L.M., Stechmann, S.N. & Martin, J.E. (2019) Balanced and unbalanced components of moist atmospheric flows with phase changes. *Chinese Annals of Mathematics, Series B*, 40, 1005–1038.
- Wetzel, A.N., Smith, L.M., Stechmann, S.N., Martin, J.E. & Zhang, Y. (2020) Potential vorticity and balanced and unbalanced moisture. *Journal of the Atmospheric Sciences*, 77, 1913–1931.
- Zhang, Y., Smith, L.M. & Stechmann, S.N. (2021a) Effects of clouds and phase changes on fast-wave averaging: a numerical assessment. *Journal of Fluid Mechanics*, 920, A49.
- Zhang, Y., Smith, L.M. & Stechmann, S.N. (2021b) Fast-wave averaging with phase changes: asymptotics and application to moist atmospheric dynamics. *Journal of Nonlinear Science*, 31, 1–46.
- Zhang, Y., Smith, L.M. & Stechmann, S.N. (2022) Convergence to precipitating quasi-geostrophic equations with phase changes: asymptotics and numerical assessment. *Philosophical Transactions of the Royal Society A*, 380, 20210030.

SUPPORTING INFORMATION

Additional supporting information can be found online in the Supporting Information section at the end of this article.

How to cite this article: Kooloth, P., Smith, L. M., & Stechmann, S. N. (2024).

Non-conservation and conservation for different formulations of moist potential vorticity.

Atmospheric Science Letters, 25(8), e1237. <https://doi.org/10.1002/asl.1237>